

Copper Complexes of “Superpodal” Amine Ligands and Reactivity Studies towards Dioxygen

Anna Jozwiuk,^[a] E. Alper Ünal,^[a] Stefan Leopold,^[a] John P. Boyd,^[a] Marco Haryono,^[a] Nadine Kurowski,^[a] Francisco Velazquez Escobar,^[b] Peter Hildebrandt,^[b] Jochen Lach,^[c] Frank W. Heinemann,^[d] Dennis Wiedemann,^[a] Elisabeth Irran,^[a] and Andreas Grohmann*^[a]

Keywords: Tetrapodal pentadentate ligands / Copper / Dioxygen / Tyrosinase-like activity / N ligands / Density functional calculations

The results of studies focussed on copper complexes of a variety of ligands with an NN₄ donor set are reported. The permethylated tetrapodal ligand **2** forms a complex with copper(I) which, upon reaction with dioxygen at –90 °C, yields a product having a bis(μ-oxido)dicopper(III) core (“O-type” product, **10**), as inferred from UV/Vis and resonance-Raman spectroscopic data. The UV/Vis spectrum of **10** has two bands at 300 and 404 nm, with extinction coefficients of 9400 and 10400 L mol⁻¹ cm⁻¹, respectively. Resonance-Raman spectra display two ¹⁶O/¹⁸O-sensitive bands which, based on the isotopic shifts and the absolute frequencies, are attributed to the Cu–O stretching modes of the O-type product. Complex **10** shows tyrosinase-like activity, as its reaction with sodium *p*-tert-butylphenolate at –90 °C in THF yields *p*-tert-butylcatechol, in an *ortho*-hydroxylation reaction (yield: 30 %). Two new rigid tetrapodal pentadentate ligands (the “superpods” **3** and **4**) can be synthesized by condensation of the primary polyamine **1** with paraformaldehyde. Their cop-

per(II) complexes (**5** and **6**) have been spectroscopically characterized. As ascertained by X-ray crystallography, **5** has the Cu^{II} ion in a tetragonal-pyramidal environment, with almost uniform Cu–N bond lengths (basal bonds: 2.052 Å and 2.070 Å; apical bond: 2.077 Å). No significant Jahn–Teller distortion is observed here. In **6**, the ligand acts as a multinucleating donor, which leads to the formation of a ladder-like cluster of [Cu(μ₃-OH)] units containing a total of two ligands, six copper(II) ions, four hydroxido ligands and eight trifluoroacetate ions. Two of the trifluoroacetate ions are non-coordinating. Variable-temperature magnetic susceptibility data are reported for this hexanuclear copper(II) cluster. Copper(I) complexes of **1** and **3** have been characterized and allowed to react with molecular oxygen, which caused the decomposition of the complexes. The IR spectra of the oxygenation products have bands at 1652 and 1632 cm⁻¹, respectively, which are absent in the spectra of **1** and **3**, suggesting that amine functions have been oxidized to imines.

Introduction

Copper has a particularly rich coordination chemistry, owing to different structural preferences of the di- and monovalent states (Cu^{II}: six-, five- or four-coordinate, often tetragonal; Cu^I: four-coordinate, tetrahedral).^[1] Because of the operation of the Jahn–Teller effect in its octahedral complexes, copper(II) has been termed a coordination chemical chameleon,^[2] with a “plasticity effect” in its stereochemistry.^[3] The biological role of copper is essentially twofold (with some parallels to that of iron): The metal atom serves as an electron relay (Cu^{I/II}) when embed-

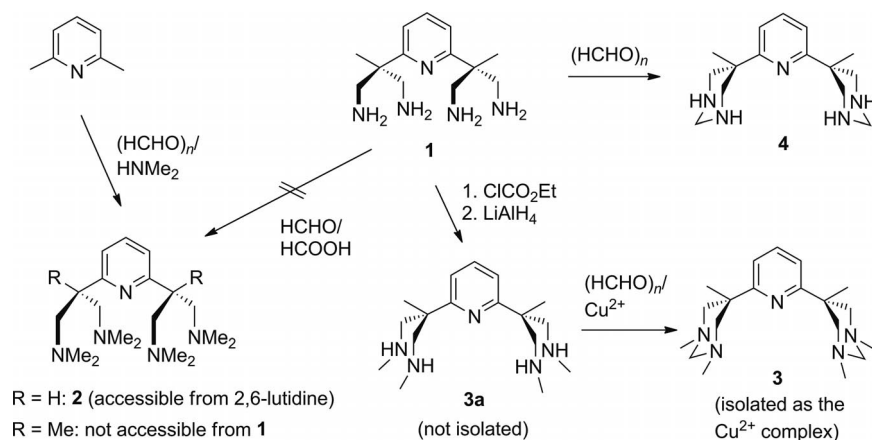
ded in specialized polypeptides (e.g. plastocyanin in photosynthesis), or is the active-site ion (Cu^{I/II} and possibly also Cu^{III}) in proteins interacting with dioxygen and its metabolites.^[4,5] Dinuclear examples where the two metal ions work in concert with one molecule of dioxygen are the oxygen carrier haemocyanin and oxidase or oxygenase enzymes such as tyrosinase.^[6,7] The latter catalyzes the *ortho*-hydroxylation of phenols to catechols (monophenolase reactivity), as well as the oxidation of catechols to *ortho*-quinones (diphenolase activity). A functional catalytic tyrosinase model has recently been described.^[8] Dinuclear dioxygen-activating enzymes in which the metal ions function largely independently of each other include dopamine-β-monooxygenase and peptidylglycine-α-hydroxylating monooxygenase. Model complexes for these enzymes are difficult to synthesize but have been reported.^[9,10] Copper sites are often used to illustrate the significance of an “entatic state” during metalloprotein function: The highly specialized polypeptide chain, which provides the metal coordination environment, is so rigid that a change in the redox state of the copper ion, as a consequence of electron transfer and/or substrate

[a] Institut für Chemie, Technische Universität Berlin, Straße des 17. Juni 135, 10623 Berlin, Germany

E-mail: andreas.grohmann@chem.tu-berlin.de
[b] Max-Volmer-Institut für Biophysikalische Chemie, Technische Universität Berlin,

Straße des 17. Juni 135, 10623 Berlin, Germany
[c] Institut für Anorganische Chemie, Universität Leipzig, Johannisallee 29, 04103 Leipzig, Germany

[d] Institut für Anorganische Chemie, Universität Erlangen-Nürnberg, Egerlandstraße 1, 91058 Erlangen, Germany



Scheme 1. Preparation of the ligands used in this study. Copper(II) complexes were obtained with ligands **3** and **4**; the copper(II) complex of ligand **1** is described in ref.^[13] The methyl groups in **2** make the ligand sterically too encumbered to give a complex with copper(II) in which the NN_4 ligand would act as a square-pyramidal coordination cap. Copper(I) complexes were obtained with ligands **1**, **2** and **4**. The condensation reaction $\mathbf{3a} \rightarrow \mathbf{3}$ is not amenable to copper(I) templating (see also text).

coordination, cannot lead to significant structural reorganization. This produces an “energetically charged state” (a “rack” state) close to the transition state of the reaction, enabling fast electron transfer and/or efficient catalysis.^[11]

Against this background, we have investigated the copper(I) and copper(II) coordination chemistry of a series of polypodal nitrogen donor ligands, based on the tetrapodal pentadentate motif **1** pioneered by our group (Scheme 1).^[12,13] We have specifically studied the reactivity of the obtained copper(I) complexes towards dioxygen. Depending on whether the ligands are permethylated or contain primary or secondary amine functions, their copper(I) complexes, upon reaction with dioxygen, produce a bis(μ -oxido)dicopper(III) complex, or imine species. The series of ligands encompasses coordination caps of variable rigidity, or “juxtapositional fixedness”,^[14] which have been obtained from the condensation of **1** with formaldehyde under a variety of conditions. Ligands and complexes have been characterized by spectroscopic techniques (NMR, IR, UV/Vis, resonance-Raman, as applicable), as well as X-ray structure analysis.

Results and Discussion

Ligand Syntheses and Structures

The ligands were prepared as shown in Scheme 1. To the best of our knowledge, the tertiary polyamine **2** has not previously been employed in a coordination chemical study. The ligand (systematic name: 2-{6-[1,3-bis(dimethylamino)propan-2-yl]pyridin-2-yl}- N^1, N^1, N^3, N^3 -tetramethylpropane-1,3-diamine) may be obtained from 2,6-lutidine (2,6-dimethylpyridine), paraformaldehyde and dimethylamine hydrochloride in a Mannich reaction,^[15] from which it is isolated as the tetrahydrochloride dihydrate. Slow cooling of a saturated aqueous solution yields single-crystalline material of composition $\mathbf{2} \cdot 4\text{HCl} \cdot 2\text{H}_2\text{O}$. The solid-

state structure of $[\text{H}_4\mathbf{2}]^{4+}$ is shown in Figure 1 (space group $Pnma$). The protons on all crystallographically independent dimethylamino groups were located in difference Fourier maps. Their charge is balanced by chloride counterions, which leads to 4 equiv. of HCl in the structure. The pyridine nitrogen atom is unprotonated, reflecting the lower basicity of pyridines when compared with aliphatic amines.^[16–18] Both 1,3-diaminoprop-2-yl moieties are in a W-like conformation, and there is a C_2 axis along the C1–N1 vector. Solvent water (one crystallographically independent molecule) was treated with fixed-distance and fixed-angle constraints. This molecule (O1) and a chloride ion (Cl3; on a general position) are in hydrogen-bonded contact, forming an infinite zigzag chain throughout the structure. The other types of chloride ions (Cl1 and Cl2; each positioned on a crystallographic mirror plane) are each hydrogen-bonded in pincer fashion by pairs of ammonio substituents, above and below the pyridine ring plane. There are no other intra- or inter-

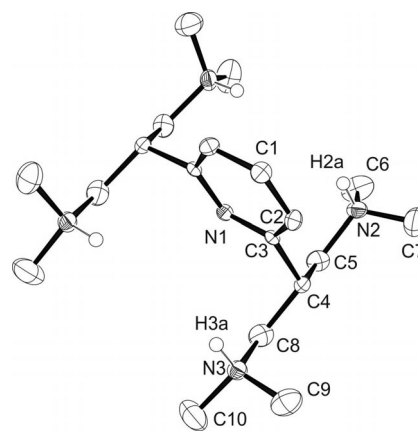


Figure 1. Crystal structure of $\mathbf{2} \cdot 4\text{HCl} \cdot 2\text{H}_2\text{O}$ (ORTEP representation, ellipsoids at the 50% probability level; N -bonded hydrogen atoms are given an arbitrary radius; other hydrogen atoms, chloride ions and water molecules are omitted for clarity).

molecular hydrogen-bonded contacts. Crystallographic data are given in Table 3.

For use in complexation studies, **2** is readily released from its HCl adduct by treatment of the latter with 4 equiv. of sodium methoxide in methanol, and subsequent removal of insoluble NaCl. Ligand **2** is structurally related to the primary polyamine **1**, whose attempted permethylation posed unexpected problems. Treatment of **1** with a mixture of formaldehyde and formic acid (i.e. the attempted reductive methylation of **1** according to Eschweiler and Clarke) invariably induced cleavage of one C–C bond at each quaternary carbon atom, in the sense of a retro-Manich reaction.^[19–21] The loss of two CH₂NH₂ groups leads to the formation of a bis(dimethylamino) imine species.^[22]

Ligand **3** {systematic name: hexahydro-5-[6-(hexahydro-1,3,5-trimethylpyrimidin-5-yl)pyridin-2-yl]-1,3,5-trimethylpyrimidine} was generated in a sequence of reactions (including metal-templated condensation) and has so far not been isolated (Scheme 1). Monomethylation of all primary amine functions in **1** is achieved by generating the tetrakis(carbamate) with ethyl chloroformate, and subsequent reduction with lithium aluminium hydride.^[23] The purification of the crude product **3a** (*N*¹,*N*³,2-trimethyl-2-[6-[2-methyl-1,3-bis(methylamino)propan-2-yl]pyridin-2-yl]-propane-1,3-diamine) by distillation or column chromatography proved impractical, and the material was therefore used directly, in a copper(II)-templated condensation with paraformaldehyde, to obtain the copper(II) complex of **3** (see the following section).

Ligand **4** {hexahydro-5-[6-(hexahydro-5-methylpyrimidin-5-yl)pyridin-2-yl]-5-methylpyrimidine} was obtained by condensation of **1** with paraformaldehyde in methanol (Scheme 1). It is necessary to control the amount of aldehyde used in this reaction as an excess leads to the formation of byproducts through the additional hydroxymethylation of one or two secondary amine functions in the desired product.^[24] Under suitable conditions (see Experimental Section), we were able to obtain pure **4** as a crystalline material. The solid-state structure of this bis(hexahydropyrimidine) derivative is shown in Figure 2 (see Table 3 for crystallographic data).

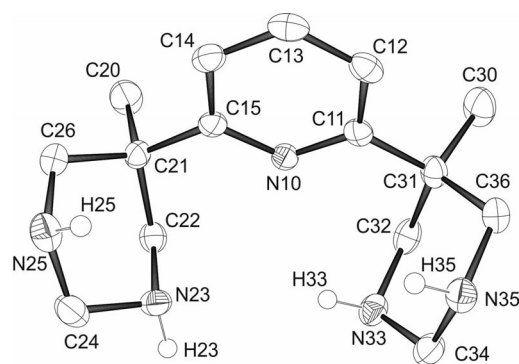


Figure 2. Crystal structure of **4** (ORTEP representation, ellipsoids at the 50% probability level; N-bonded hydrogen atoms are given an arbitrary radius; other hydrogen atoms are omitted for clarity).

Both hexahydropyrimidine (hhp) rings are in the chair conformation. There is a weak intramolecular hydrogen bond between the aminal NH group (involving N35) of one hhp ring and the pyridine nitrogen atom N10 [N35–H35...N10 2.975(2) Å, 120.6(13)°]. The relative orientation of the N–H bonds in both hhp rings is notable. While one ring has both hydrogen atoms in axial positions (H33, H35), the other has one hydrogen atom in an equatorial and the other in an axial position (H23 and H25, respectively). For hexahydropyrimidines, the theory predicts the axial/axial (*aa*) and axial/equatorial (*ae*) conformations to be favoured over the *ee* conformation. The former two conformers are of nearly the same energy, with $n_{\text{N}}-\sigma^*(\text{C}-\text{N})$ hyperconjugation favouring *aa* slightly over *ea*. The *ee* conformer is the least stable owing to 1,3-dipolar repulsion between the axial lone pairs on the nitrogen atoms.^[25] In the case of **4**, the availability of the pyridine nitrogen atom for hydrogen bonding is expected to have an influence on the conformation of at least one of the hhp rings. Both ligands **3** and **4** may be construed as rigidified variants of the NN₄ ligand **1**, in which the 1,3-diaminoprop-2-yl side arms have been made into rings by the introduction of methylene bridges, to counter the "plasticity effect" of copper(II) mentioned in the Introduction, and thereby perhaps elicit unusual reactivity.

Complex Syntheses and Properties

[Cu^{II}(**3**)](ClO₄)₂ (**5**)

Crude **3a** was treated with paraformaldehyde in methanol, in the presence of hexakis(dimethylformamide)-copper(II) perchlorate. Two variants were tested: paraformaldehyde was added to a solution of preformed complex {**3a** + [Cu(dmf)₆](ClO₄)₂}, or a solution of **3a** and paraformaldehyde was treated with the copper salt, added as a solid. In both cases, and within minutes, the reaction mixture deposited a blue precipitate, which was collected and recrystallized from methanol to obtain single crystals of **5** suitable for an X-ray structure determination (Figure 3). A selection of bond lengths and angles is given in Table 1, and crystallographic data are listed in Table 3.

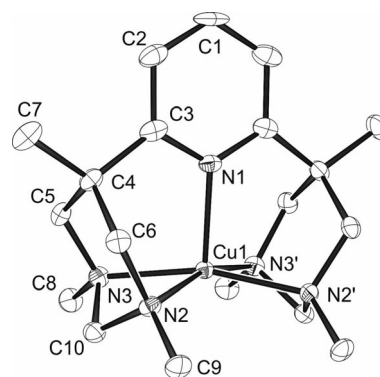


Figure 3. Crystal structure of **5** (ORTEP representation, ellipsoids at the 50% probability level; hydrogen atoms and perchlorate counterions are omitted for clarity).

FULL PAPER

Table 1. Selected bond lengths [Å] and bond angles [°] for **5**.

Bond length or angle		Bond length or angle	
Cu1–N1	2.077(4)	N2–Cu1–N2'	109.1(2)
Cu1–N2	2.052(3)	N2–Cu1–N3	66.9(1)
Cu1–N3	2.070(3)	N2–Cu1–N3'	163.6(1)
N1–Cu1–N2	98.0(1)	N3–Cu1–N2'	163.6(1)
N1–Cu1–N2'	98.0(1)	N2'–Cu1–N3'	66.9(1)
N1–Cu1–N3	98.4(1)	N3–Cu1–N3'	112.1(1)
N1–Cu1–N3'	98.4(1)		

The copper(II) ion in **5** is coordinated in a tetragonal-pyramidal fashion, with five Cu1–N bonds of similar lengths [Table 1; average: 2.064(3) Å]. The molecule has a mirror plane orthogonal to the pyridine ring, containing the atoms C1, N1 and Cu1. The hhp rings lock the NN₄ donor arrangement in place, resulting in symmetrical coordination of the copper ion. The six-membered rings with their attendant ring strain (chair conformation) apparently cause the copper ion to move towards the pyridine nitrogen atom, above the basal N₄ plane. Consequently, no Jahn–Teller elongation is observed here, in contrast to the complex [Cu(1)](SCN)₂·H₂O, which contains the more flexible parent tetraaminoimine **1** as a square-pyramidal capping ligand [Cu–N_{ax} 2.207(2) Å vs. Cu–N_{bas} av. 2.039(3) Å].^[13]

**[Cu^{II}₆(4)₂(μ-CF₃CO₂)₂(CF₃CO₂)₄(H₂O)₂(μ₃-OH)₄]-
(CF₃CO₂)₂·6MeOH·2H₂O (**6**)**

None of the complexation reactions undertaken with **4** and a variety of copper(II) salts produced single crystals of mononuclear complexes that would have enabled a structural comparison with the complexes of ligands **1** and **3**. [Cu(dm_f)₆](ClO₄)₂ and CuCl₂ in methanol were the first salts used. The formation of complexes was indicated by colour changes (typically to blue or green), the formation of precipitates and confirmed by mass spectrometry. Anion exchange was tried in order to obtain single crystals, and a solution of a silver salt AgX (X = BF₄, SbF₆, CF₃SO₃, CF₃CO₂) in methanol added dropwise to a solution of the copper(II) chloride complex in the same solvent. The precipitation of AgCl was spontaneous in all cases, the colour of the solution changing from green to blue. AgCl was removed by filtration, and the filtrate was used for crystallization by slow concentration, by diethyl ether diffusion or by layering of the methanol solution with diethyl ether. Only in the case with trifluoroacetate as the counterion did these procedures produce single crystals suitable for X-ray diffraction. The structure (Figures 4 and 5) is oligonuclear, containing a ladder-like cluster of [Cu(μ₃-OH)] units with a total of two ligands, six copper(II) ions, four hydroxido ligands and eight trifluoroacetate ions, as well as two water and six methanol molecules per unit cell. As water was not purposely added to the mother liquor, the hydroxido ligands and solvate water molecules must derive from moisture introduced through the solvents or the metal salts used.

The structure of **6** is centrosymmetric. Each ligand coordinates to three copper ions (Cu1, Cu2 and Cu3). One of the metal ions, Cu1, is connected to the pyridine nitrogen atom N10 of one of the chelate ligands and to one nitrogen

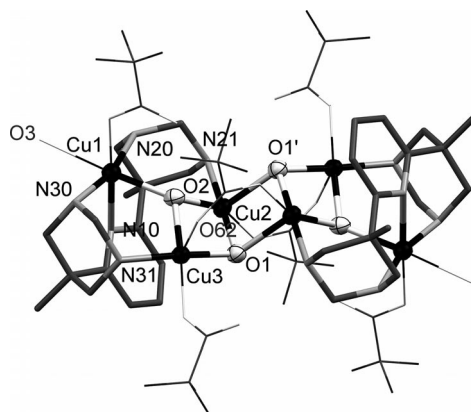


Figure 4. Crystal structure of **6** (MERCURY representation). The Cu–O core is rendered in ellipsoid (90% probability level), N donor ligands are in stick and all other ligands in wireframe representations (disordered groups in one representative position). Hydrogen atoms, trifluoroacetate counterions and solvent molecules are omitted for clarity.

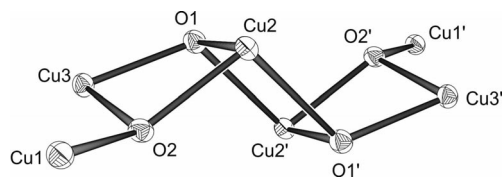


Figure 5. Detail of the crystal structure of **6** in ORTEP representation (Cu–O coordination core, ellipsoids at the 50% probability level).

atom of each of its diazacyclohexyl rings (N20 and N30). The other two nitrogen atoms of the ligand (one in each diazacyclohexyl ring, N21 and N31) are coordinated to the copper ions Cu2 and Cu3, respectively. Cu1 is six-coordinate quasi-octahedral with the three N donors already mentioned, one hydroxido, one trifluoroacetato-κ¹O and one aqua ligand. The bond lengths (Table 2) range from 1.963(1) to 2.230(1) Å, except for the bond Cu1–O3 which, at 2.472(1) Å, is considerably longer. Cu2 and Cu3 are each coordinated in a square-pyramidal fashion and together with the bridging hydroxido ligands (O1 and O2) create the ladder-like backbone. The lengths of the basal bonds are in the range 1.949(2)–2.016(2) Å (for Cu2) and 1.937(2)–2.028(2) Å (for Cu3), whereas the apical donors O1' (in the case of Cu2) and O62 (Cu3) are bonded to Cu^{II} at a greater distance [2.289(2) and 2.279(2) Å, respectively], owing to the Jahn–Teller effect. Finally, the ions in the pairs Cu2/Cu3' and Cu2'/Cu3 are connected by bridging μ-trifluoroacetato ligands.

Structures containing similar [Cu(μ₃-OH)] clusters have been reported,^[26–29] with [Cu₂(OH)₂] repeating units making up cube- or ladder-like entities. A complex described by Zheng and co-workers^[30,31] contains a zigzag chain whose overall structural pattern, as well as bond lengths and angles, are similar to that of **6**. Complex **6** is different in that it has extra copper atoms, Cu1 and Cu1', which are joined to the rest of the cluster by only one Cu–(μ₃-OH) bond. The formation of **6** is reproducible, and its targeted

Table 2. Selected interatomic distances [Å] and bond angles [°] for **6**.

Bond length or angle		Bond length or angle	
Cu1–N10	2.230(1)	N10–Cu1–O2	83.8(1)
Cu1–N20	1.963(1)	N20–Cu1–O2	95.0(1)
Cu1–N30	1.964(1)	N30–Cu1–O2	99.2(1)
Cu2–N21	2.016(2)	N10–Cu1–O3	102.3(1)
Cu3–N31	2.028(2)	N20–Cu1–O3	86.4(1)
Cu1–O2	2.158(1)	N30–Cu1–O3	79.1(1)
Cu1–O3	2.472(1)	N10–Cu1–O50	178.1(1)
Cu1–O50	2.135(1)	N20–Cu1–O50	88.5(1)
Cu2–O1	1.949(2)	N30–Cu1–O50	85.6(1)
Cu2–O2	1.991(2)	O2–Cu1–O50	97.7(1)
Cu2–O1'	2.289(2)	O3–Cu1–O50	76.1(1)
Cu2–O40	1.979(2)	O2–Cu1–O3	173.7(1)
Cu3–O1	1.937(2)	O1–Cu2–O2	81.55(6)
Cu3–O2	1.988(2)	O1–Cu2–O1'	85.72(6)
Cu3–O61	1.972(2)	O2–Cu2–O1'	101.05(6)
Cu3–O62	2.279(2)	O2–Cu3–O1	81.93(6)
N10–Cu1–N20	92.6(1)	Cu2–O1–Cu3	97.33(7)
N10–Cu1–N30	93.0(1)	Cu2–O2–Cu3	94.33(6)
N20–Cu1–N30	165.3(1)	Cu2–O1–Cu2'	94.28(6)
Cu1–Cu3	3.622(2)	Cu1–O2–Cu3	121.75(7)
Cu2–Cu3	2.918(2)		
Cu2–Cu2'	3.115(2)		

synthesis was accomplished as described in the Experimental Section.

Temperature-dependent susceptibility measurements on a powdered sample of **6** were carried out by using a SQUID Magnetometer (MPMS 7 XL, Quantum Design) over the temperature range 2–371 K in an applied external field of 0.5 T. Figure 6 shows the variation of the molar susceptibility χ_m and the effective magnetic moment μ_{eff} with temperature. The value of μ_{eff} decreases slowly from 4.47 μ_B at 371 K to 4.10 μ_B at 100 K and then more steeply on further cooling, reaching a minimum of 1.91 μ_B at 2 K. The effective magnetic moment of **6** at room temperature (4.41 μ_B) is much smaller than the theoretical spin-only value of 6.93 μ_B calculated for six uncoupled Cu^{II} ions ($S = 3$, $S_i = 1/2$, $g = 2.00$), indicative of net antiferromagnetic exchange interactions and an $S = 0$ ground state.

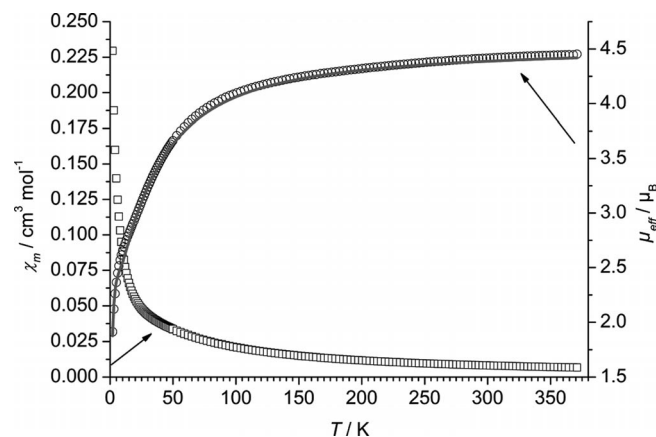


Figure 6. Plots of χ_m (squares) and μ_{eff} (circles) vs. T for the hexanuclear copper(II) complex **6**. The solid line represents the best fit.

The magnitude of the exchange interactions was determined by least-squares fitting of the experimental magnetic

susceptibility data to the isotropic HDvV exchange Hamiltonian [Equation (1)] using a full-matrix diagonalization approach.^[32] In a first attempt, we tried to simulate the experimental data on the basis of a tetranuclear unit with two noncorrelated copper(II) ions, by assuming $J_3 = 0 \text{ cm}^{-1}$ as suggested for a similar complex by Li et al.^[30,31] This attempt reproduced the experimental data reasonably well over the temperature range 20–371 K for $J_1 = -27 \text{ cm}^{-1}$, $J_2 = -25 \text{ cm}^{-1}$ and $g = 2.15$, but failed at lower temperatures. The introduction of a third exchange coupling constant ($J_3 \neq 0 \text{ cm}^{-1}$) significantly improved the model, leading to a good fit over the whole temperature range, with $J_1 = -23 \text{ cm}^{-1}$, $J_2 = -29 \text{ cm}^{-1}$, $J_3 = -5 \text{ cm}^{-1}$ and $g = 2.16$ (Figure 7). The fact that J_3 (at -5 cm^{-1}) is significantly smaller than the other two exchange coupling constants, J_1 and J_2 , can be rationalized by the fact that the distance of the Cu spin centres giving rise to J_3 is the largest, the distances associated with J_1 and J_2 being shorter by 0.5 Å and 0.7 Å, respectively.

$$\hat{H} = -2J_1(\hat{S}_2 \cdot \hat{S}_3 + \hat{S}_4 \cdot \hat{S}_5) - 2J_2(\hat{S}_3 \cdot \hat{S}_4) - 2J_3(\hat{S}_1 \cdot \hat{S}_2 + \hat{S}_5 \cdot \hat{S}_6) \quad (1)$$

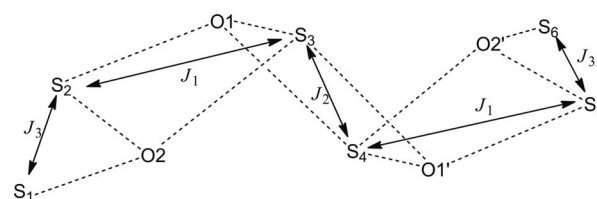


Figure 7. Core structure of **6** with exchange coupling pathways (double arrows) J_1 , J_2 and J_3 (see also Figure 5). In this model J_1 represents the sum of two coupling pathways (through the O1 and O2 oxido bridges).

[Cu^I(1)](PF₆) (**7**)

Complex **7** is generated by the reaction of tetrakis(ace-tonitrile)copper(I) hexafluorophosphate with **1** in THF, and precipitates from solution as light-yellow prism-shaped crystals upon diffusion of diethyl ether. In the ¹H NMR spectrum of **7** ([D₆]DMSO, room temp.), all resonances show a complexation-induced shift to low field as compared to the signals of the free ligand, while the overall appearance of the NMR spectrum suggests a highly symmetrical cation structure. Specifically, the methylene groups give rise to an AB spin system, indicating the geminal protons to be diastereotopic. This is compatible with either a square-pyramidal coordination geometry (in which all five N donors of the chelate ligand are bonded to Cu^I; C_{2v}) or a tetrahedral set of N donors around Cu^I. The latter, which reflects the coordination chemical preference of copper(I), would involve a coordination/decoordination process that is fast on the NMR timescale, in which the pyridine N atom and three out of the four primary amine N atoms are coordinated to the metal centre at any one time. The complex is extremely sensitive towards dioxygen. Even the most exacting precautions to exclude air during single-crystal X-ray diffraction could not prevent the crystals from taking on a bluish hue in the process. The quality of the structure

determination is, however, acceptable. In the solid state, **7** is a coordination polymer, with monovalent copper (Cu1) in a distorted tetrahedral environment (Figure 8). The metal ion is coordinated by three nitrogen donors (N1, N3 and N4) of one pentadentate ligand and a fourth donor (N2) that belongs to a second ligand. One of the primary amine functions of the first ligand (N5) remains uncoordinated. The Cu1–N(amine) bond lengths lie in the range 2.0–2.1 Å [Cu1–N4 1.999(5) Å, Cu1–N2 2.042(5) Å, Cu1–N3 2.105(5) Å], while the bond to the pyridine nitrogen atom N1 is significantly longer [Cu1–N1 2.372(5) Å]. There are weak intra- and intermolecular hydrogen-bonded contacts between the primary amine nitrogen atoms N4 and N5 and between N3/N4/N5 and the hexafluorophosphate counterion. Crystallographic data for **7** are given in Table 3.

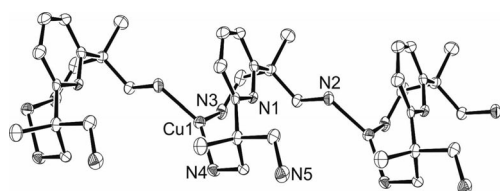


Figure 8. Section of the 1D coordination polymer in **7** (ORTEP representation; ellipsoids at the 50% probability level; hydrogen atoms and hexafluorophosphate counterion are omitted for clarity).

[Cu^I(**2**)](PF₆) (**8**)

Complex **8** was obtained by the reaction of ligand **2** with tetrakis(acetonitrile)copper(I) hexafluorophosphate in THF. Combining the colourless reactants immediately produced a yellow-orange solution, with only very little precipitate after 3 h. Removal of the solvent in vacuo left a green-brownish solid. Elemental analysis data are consistent with the chemical formula of **8** (C₁₉H₃₇CuF₆N₅P), and ESI-MS data indicate a mononuclear complex in the gas phase (*m/z* = 398.2337 [Cu(**2**)⁺]). When compared to the ¹H NMR spectrum of the free ligand, coordination shifts the resonances to low field ([D₆]DMSO, room temp.). The protons on the pyridine ring give rise to an AB₂ spin system and show a triplet (δ = 7.84 ppm; 1 H, *para*) and a doublet (δ = 7.27 ppm; 2 H, *meta*). The chemical shifts of the methylene protons (AB system; the geminal protons are diastereotopic) are δ = 2.65 and 2.54 ppm, respectively. The aliphatic methine protons (δ = 3.16 ppm) give rise to a higher-order multiplet from the coupling to the adjoining CH₂ groups. The methyl groups on the nitrogen atoms are magnetically equivalent as only one singlet is observed in the ¹H NMR spectrum. This suggests exchange (rapid on the NMR timescale at room temperature) of the coordinating NMe₂ residues. Structures of complexes with permethylated propane-1,3-diamine and related ligands have been discussed in the literature, with special consideration of the

Table 3. Crystallographic data for compounds **2**·4HCl·2H₂O, **4**, **5**, **6**·6MeOH·2H₂O and **7**.

	2 ·4HCl·2H ₂ O	4	5	6 ·6MeOH·2H ₂ O	7
Empirical formula	C ₁₉ H ₄₅ Cl ₄ N ₅ O ₂	C ₁₅ H ₂₅ N ₅	C ₁₉ H ₃₃ Cl ₂ CuN ₅ O ₈	C ₅₂ H ₈₆ Cu ₆ F ₂₄ N ₁₀ O ₃₀	C ₁₃ H ₂₅ CuF ₆ N ₅ P
<i>M_r</i> [g mol ⁻¹]	517.40	275.40	593.94	2168.61	459.89
Crystal system	orthorhombic	triclinic	orthorhombic	triclinic	monoclinic
Space group	<i>Pnma</i>	<i>P1</i>	<i>Pnma</i>	<i>P1</i>	<i>P2₁/c</i>
<i>a</i> [Å]	12.0211(3)	8.1936(5)	22.9754(9)	12.2860(4)	6.3188(9)
<i>b</i> [Å]	21.5002(4)	9.9327(6)	12.2587(6)	12.3193(3)	22.669(2)
<i>c</i> [Å]	10.4549(2)	10.5803(5)	8.6635(4)	15.1404(4)	12.4931(4)
α [°]	90	65.062(5)	90	84.364(2)	90
β [°]	90	80.856(4)	90	80.382(2)	90.947(6)
γ [°]	90	78.633(5)	90	62.607(3)	90
<i>Z</i>	4	2	4	1	4
<i>V</i> [Å ³]	2702.13(10)	762.69(7)	2440.06(19)	2005.43(11)	1789.3(3)
ρ_{calcd} [mg cm ⁻³]	1.272	1.199	1.617	1.796	1.707
Diffractometer	Oxford Xcalibur S	Oxford Xcalibur S	Oxford Xcalibur S	Oxford Xcalibur S	Bruker–Nonius Kap-paCCD
λ [Å]	0.71073	0.71073	0.71073	0.71073	0.71073
Crystal size [mm]	0.24 × 0.15 × 0.14	0.25 × 0.23 × 0.13	0.15 × 0.12 × 0.06	0.24 × 0.23 × 0.21	0.20 × 0.16 × 0.14
<i>T</i> [°C]	150(2)	150(2)	150(2)	150(2)	150(2)
Absorption correction	multi-scan	multi-scan	multi-scan	multi-scan	multi-scan
<i>T_{max}</i> / <i>T_{min}</i>	1.00000/0.93833	1.00000/0.95462	1.00000/0.93020	1.00000/0.94096	0.825/0.687
Scan	ω	ω	ω	ω	ω and ϕ
2θ range [°]	3.20 ≤ 2θ ≤ 25.00	3.11 ≤ 2θ ≤ 25.00	3.01 ≤ 2θ ≤ 24.99	3.10 ≤ 2θ ≤ 30.00	3.60 ≤ 2θ ≤ 27.10
Measured reflections	12722	7378	11427	24972	31174
Unique reflections	2452	2682	2259	11652	3918
Observed reflections	2066	2251	1759	8926	3334
μ (Mo– <i>Kα</i>) [mm ⁻¹]	0.462	0.075	1.169	1.702	1.378
Refined parameters	158	199	175	578	238
Data/parameter ratio	15.5	13.5	12.9	20.2	16.5
<i>wR</i> ₂ (all data)	0.1772	0.0859	0.0825	0.0813	0.1943
<i>R</i> ₁ (obsd. data)	0.0864	0.0351	0.0467	0.0344	0.0678
ρ_{fin} (max/min) [e Å ⁻³]	1.142/–0.376	0.214/–0.146	0.376/–0.708	0.727/–0.622	1.053/–0.705

steric bulk introduced by the dimethylamine donor groups.^[33–35] In solution, at room temperature, the observation of one singlet in the ¹H NMR spectrum for the *N*-bonded methyl groups leads us to presume fast averaging of the four tertiary amine donors, of which three are coordinated at any one time, resulting in a tetrahedral or trigonal-pyramidal coordination geometry around copper(I). Single crystals of **8** have not been obtained so far. DFT calculations for complex **8** are compatible with an overall trigonal-pyramidal coordination geometry in the gas phase, as depicted in Figure 9.

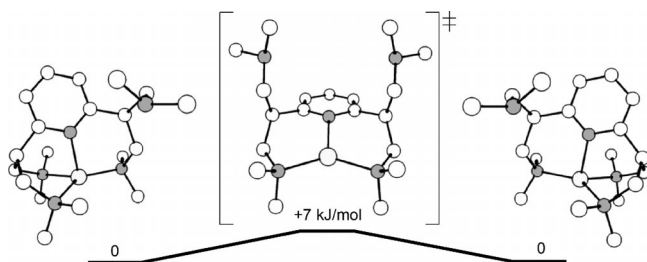


Figure 9. Gas-phase structures of $[\text{Cu}(\mathbf{2})]^+$ (DFT). A similar averaging process is suggested to operate in solution, explaining the equivalence of the NMe_2 groups as observed by ¹H NMR spectroscopy at room temperature.

To support our assumption, DFT calculations on the RB3LYP/DGDZVP level were performed by using the Gaussian 03 (C02) program package. There are two different stable conformations differing in energy by 13 kJ mol⁻¹ and arising from a subtle conformation change. The more favourable conformer is characterized by a displacement (0.1 Å) of the copper ion from the plane defined by the three coordinating tertiary amine donors. The coordination geometry around copper(I) is, therefore, best described as distorted trigonal-pyramidal, not tetrahedral. The high symmetry suggested by the ¹H NMR spectrum

requires the interconversion/enantiomerization of these asymmetric (C_1) structures at room temperature. An intermediate geometry is expected to exist (a stable geometry or a transition state) that is achiral and lies sufficiently low in energy. We located a possible tricoordinate transition state that fulfils this requirement, as its approximate symmetry group is C_s . This transition structure is only 7 kJ mol⁻¹ higher in energy than the more favourable conformer, and thus lower in energy than the less favourable conformer. We conclude that, because of steric strain, coordination of three out of four dimethylamino donors in **8** is not accompanied by a significant energy gain in comparison to coordination of two out of four dimethylamino donors, yet this may occur in the gas phase where no additional monodentate donors (solvent molecules) are present. In a coordinating solvent (such as DMSO, THF, acetonitrile), it appears reasonable that **2** acts as a tridentate ligand with the remaining coordination site on copper(I) occupied by a solvent molecule.

To support the results obtained by DFT calculations, we carried out variable-temperature (VT) ¹H NMR spectroscopic measurements (between room temperature and 180 K). Three solvents with sufficiently low melting points were tested, $[\text{D}_6]$ acetone, $[\text{D}_4]$ methanol and $[\text{D}_8]$ tetrahydrofuran. While complex **8** is stable in all of these solvents (provided they are strictly oxygen-free), its solubility is low in all cases. We specifically note that **8** is not per se unstable in protic solvents, such as methanol. The best results were obtained with $[\text{D}_8]$ tetrahydrofuran. Upon lowering of the temperature, there is overall line broadening. The position of the aromatic proton resonances is unaffected; the resonances belonging to the NMe_2 methyl groups split at very low temperature, but overlap extensively; the methylene resonances move to higher field and start to overlap with the broadened NMe_2 methyl resonances. The only signal we found useful as a low-temperature probe of the mo-

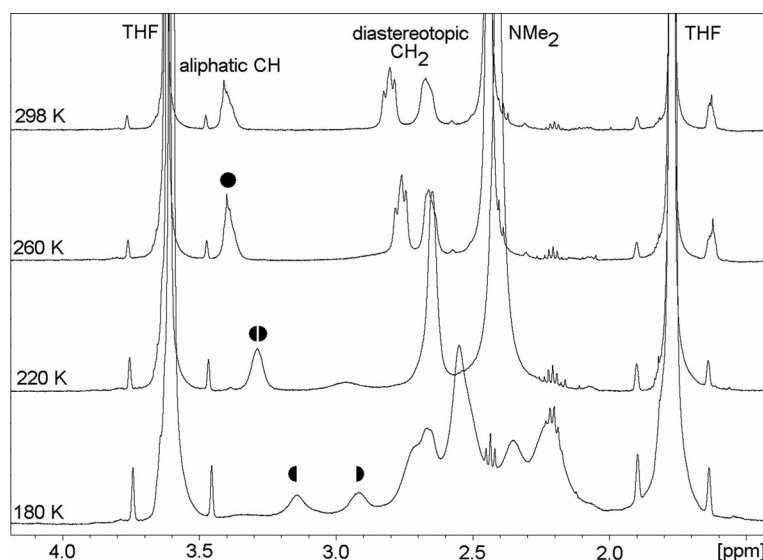


Figure 10. Partial VT NMR spectra of **8** in $[\text{D}_8]$ THF (see text).

lecular dynamics is the methine signal belonging to the bridgehead CH moieties in the ligand side arms. This signal splits into two clearly differentiated resonances at $-93\text{ }^{\circ}\text{C}$ (180 K) in spite of the observed line broadening. The following behaviour is to be expected on the basis of the DFT model: If two enantiomeric forms of the copper(I) complex are in rapid equilibrium, six of the eight NMe_2 methyl groups (belonging to the three dimethylamino groups coordinated to the copper ion) will be chemically inequivalent. Uncoordinated NMe_2 will give rise to one additional signal. The methylene protons will give rise to eight different signals (instead of two at room temperature), as each methylene group is on an arm of the ligand not symmetry-related to any other (given that enantiomerization is slow on the NMR timescale and the protons in each methylene group are diastereotopic). The methyl and methylene proton signals overlap strongly in the experimental spectrum, as expected for 15 different signals in that region. Most importantly, the methine signals would also be differentiated, as the two sides of the molecule are inequivalent in frozen equilibrium, just as the pendant arms are. This behaviour is in fact observed in the experimental spectrum (Figure 10). In summary, while the room-temperature spectrum is compatible with pseudo- C_{2v} point group symmetry of the complex, the spectrum recorded at $-93\text{ }^{\circ}\text{C}$ suggests C_1 symmetry. Thus, the VT ^1H NMR spectroscopic data are fully compatible with the density functional theory results described above. The low energy barrier to enantiomerization (as suggested by DFT calculations) is consistent with incomplete freezing of the equilibrium at $-93\text{ }^{\circ}\text{C}$, as inferred from the observed line width.

$[\text{Cu}(\mathbf{4})](\text{PF}_6)$ (**9**)

Complex **9** was obtained by treating a slight excess of ligand **4** with tetrakis(acetonitrile)copper(I) hexafluorophosphate in THF. The combination of the colourless reactants resulted in a yellow solution, which deposited a green-yellowish precipitate. This was filtered, washed with THF (to remove traces of the ligand) and dried in vacuo. The elemental analysis is consistent with a 1:1 complex of chemical formula $\text{C}_{15}\text{H}_{25}\text{CuF}_6\text{N}_5\text{P}$ (complex **9**). ESI-MS data indicate a mononuclear complex in the gas phase ($m/z = 338.1407$ $[\text{Cu}(\mathbf{4})]^+$). The ^1H NMR spectrum of **9** ($[\text{D}_6]$ -DMSO, room temp.) shows proton resonances which, when compared to those of the free ligand, are shifted to low field. Similar to **8**, the protons on the pyridine ring (AB_2 spin system) show a triplet ($\delta = 7.89$ ppm) and a doublet ($\delta = 7.53$ ppm). The methylene resonances (AB system) appear at $\delta = 3.68$ and 2.83 ppm, respectively. The formaldehyde-derived methylene bridges (C_1 linkers between the N atoms in the hexahydropyrimidine rings) show a broad singlet at $\delta = 3.72$ ppm, and the singlet at $\delta = 1.09$ ppm is assigned to the exocyclic methyl groups. As judged from the NMR spectra, the coordination of the metal ion in solution is most likely similar to **8**, with fast averaging of the four secondary amine N atoms, of which three are coordinated at any one time. No single crystals of compound **9** have been obtained so far.

Reactivity of the Cu^{I} Complexes towards O_2

The reactivity of complexes **7–9** towards dioxygen was studied. All three compounds are sensitive to air. While the yellowish solutions of **7** and **9** in acetonitrile immediately turn green upon exposure to air, the colour change in solutions of **8** in THF or acetonitrile (from greenish to blue) is slow and takes about 5 min at room temperature. The spectroscopic characterization of the oxygenated products was performed as follows.

Dry dioxygen was passed through a solution of **7** in acetonitrile for several minutes, which induced a colour change from light yellow to green. A high-resolution ESI mass spectrum of the resulting solution shows a peak at $m/z = 248.1864$ that can be correlated with the uncomplexed, ligand-derived species $[\mathbf{1-3H}]^+$, a protonated diimine of **1**. The simulated isotope pattern of this ion has the same peak structure. The ion is not observed in the ESI mass spectrum of a solution of **7** under inert conditions. The IR spectra of complex **7** and of its oxidation product (after exposure to O_2 ; both as KBr discs) are very similar, but an additional band appears at 1652 cm^{-1} after oxidation (a region typical of imine vibrations). We conclude from this information that the ligand in **7** is partially oxidized (primary amine to imine) upon exposure to dioxygen, and probably decoordinates at the same time. Future work will seek to provide conclusive evidence for this process, based on ^1H NMR spectroscopy. Similar reactions of copper(I) complexes containing amine hydrogen atoms (primary and/or secondary amine functions) in the presence of dioxygen have been reported in the literature.^[36,37] In a separate experiment, dry dioxygen was passed through a solution of **9** in MeCN for several minutes, which caused a colour change from light yellow to green. ESI mass spectrometry and IR spectroscopy (the reaction with O_2 causes the appearance of a new band at 1632 cm^{-1}) indicate the oxidation of complex **9** to proceed with concomitant mono- and diimine formation and decoordination, similar to that of **7**.

Of the ligands studied in this work, **2** is special in that it contains only tertiary amine donors in its periphery, which precludes imine formation in the course of oxidation. ESI mass spectra of solutions of **8** in THF, measured a few minutes after exposure to air, still show a peak attributable to the copper(I) complex $[\text{Cu}(\mathbf{2})]^+$, suggesting that the oxidation of **8** proceeds relatively slowly. In order to check for dioxygen-derived products of **8**, samples exposed to molecular dioxygen were monitored by low-temperature UV/Vis spectroscopy (solvent: THF). In the absence of dioxygen, the UV/Vis spectrum of **8** is characterized by two bands, at 330 nm (metal-to-ligand charge-transfer, MLCT) and 264 nm (ligand-centred transitions, $\pi \rightarrow \pi^*$ or $n \rightarrow \pi^*$), with extinction coefficients of 5900 and $1200\text{ L mol}^{-1}\text{ cm}^{-1}$, respectively. Upon passing dry oxygen through the cooled solution ($-90\text{ }^{\circ}\text{C}$), the colour changed from light yellow to brown. Two new bands, at 300 and 404 nm, with extinction coefficients of 9400 and $10400\text{ L mol}^{-1}\text{ cm}^{-1}$, respectively, appeared, and their intensities increased while dioxygen was being added to the solution (Figure 11). No further change

could be observed after an addition time of ca. 4 min, and the addition of dioxygen was stopped. Purging the THF solution with argon did not change any of the UV/Vis features. The cooling bath was removed, and UV/Vis spectra measured at 10 °C intervals while the solution was warmed to room temperature. The bands at 300 and 404 nm gradually disappeared, indicating that the absorbing species is very unstable at higher temperatures.

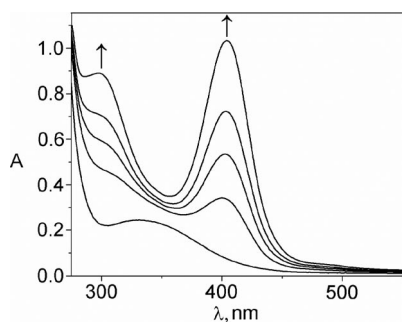


Figure 11. Spectral changes associated with the exposure of **8** to O₂ at -90 °C (the initial concentration of **8** is 2 mmol L⁻¹). Spectra were measured before the addition of O₂ ($t = 0$; lowest line, spectrum 1), immediately after addition of O₂ (spectrum 2) and then at 60 s intervals (spectra 3–5).

The reaction of copper(I) complexes with dioxygen at low temperature can produce different kinds of Cu^I/Cu^{III}-superoxido/peroxido/oxido complexes having different Cu/O ratios, depending on the nature of the supporting ligands. There is an extensive body of literature on complexes containing a Cu₂O₂ core [bis(μ-oxido)dicopper(III) and peroxido-dicopper(II), classed as **O**-type and **SP**-type complexes, respectively].^[6] **O**- and **SP**-type complexes are distinguishable from one another by their specific UV/Vis absorptions and Raman vibrations. Examples of either species have been isolated, and equilibria of interconverting **O**- and **SP**-type complexes are also well documented.^[38,39] In our case, it is reasonable to assume that a single, well-defined species (**10**) is formed upon reaction of **8** with dioxygen, and the UV/Vis features described above are characteristic of an **O**-type copper/dioxygen product, containing a bis(μ-oxido)dicopper(III) core.^[6,40,41] The bands at 300 nm and 404 nm may be attributed to an oxide-to-Cu^{III} charge transfer.^[42] In nonprotic solvents at -80 to -90 °C, what is presumably the complex [**8**·(O₂)] is stable for several hours. Since purging with argon does not alter the spectroscopic characteristics, dioxygen appears to be strongly bound. Its removal under vacuum was not attempted. At temperatures above -80 °C, compound **10** decomposes quickly.

The resonance-Raman (RR) bands of the Cu–O core are highly diagnostic of **O**-type coordination of the O₂ unit. Spectra of the products obtained with ¹⁶O₂ and ¹⁸O₂ were measured in frozen THF solution (Figure 12). The RR spectrum of the ¹⁶O-derived product shows bands at 620 and 616 cm⁻¹ that shift down to 589 and 581 cm⁻¹, respectively, in the spectrum of the ¹⁸O-derived product. The two closely spaced bands in each spectrum point to subtle structural differences between the two μ-oxido bridges of the **O**-

type core, reflected by slightly different frequencies of the Cu–O stretching vibrations. Correlating the respective high- and low-frequency components of the ¹⁶O- and ¹⁸O-derived products, one obtains very similar isotopic shifts for each conjugate band pair (31 and 35 cm⁻¹), confirming that the nature of the underlying modes is the same. The absolute frequencies and the ¹⁸O/¹⁶O shifts are in good agreement with literature values.^[6]

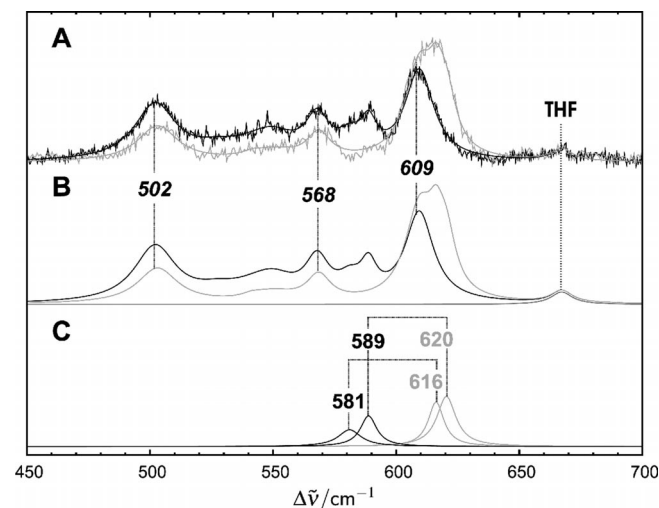


Figure 12. (A) RR spectra of the dioxygen-derived products **10**, prepared with ¹⁶O₂ (grey) and ¹⁸O₂ (black). Both spectra were normalized to the solvent band (THF). (B) Simulated spectra obtained from a fit of Lorentzian functions to the experimental spectra of the ¹⁸O₂- and ¹⁶O₂-derived products; the spectral THF contribution is displayed separately; bands insensitive to ¹⁸O₂ labelling are denoted by numbers in italics. (C) Single Lorentzian functions, referring to the Cu–O stretching modes of the experimental spectra.

Tyrosinase-Like Reactivity of the **O**-Type Species **10**

On the basis of spectroscopic data, the oxygenated active site of tyrosinase has been proposed to be a side-on peroxido-dicopper(II) core.^[40] Not all steps in the catalytic cycle of the enzyme acting as a monophenolase have been understood to date, and attempts to model the function of the active site are numerous. Several synthetic side-on peroxido-dicopper(II) complexes have shown monophenolase and sometimes additional diphenolase activity, yielding catechols and quinones, respectively. These findings have been summarized recently.^[43] It was shown for the first time in 2005 that a bis(μ-oxido)dicopper(III) intermediate can activate phenolate to yield a catechol as well as a quinone.^[44] Subsequently, a bis(μ-oxido)dicopper(III) complex was isolated and shown to react directly with the sodium salts of *para*-substituted phenolates, to give only the corresponding catechol.^[45] Similar reactivity but higher product yields, using a different bis(μ-oxido)dicopper(III) complex, were reported independently, and byproducts like quinone and in some cases bis(phenols) were also observed in this work.^[46] Selective phenolate *ortho*-hydroxylation was also shown with an asymmetric dicopper μ-η¹:η¹-peroxido complex.^[47]

We investigated the behaviour of **10** in this context. Sodium *p*-*tert*-butylphenolate (1 equiv.), dissolved in THF in one portion, was added to a solution of freshly generated **10**. UV/Vis monitoring showed the disappearance of the bands at 300 and 404 nm upon addition, indicating reaction of the oxygen–copper complex with the substrate. Acidic workup (quenching with 1 M HCl) of the warm reaction solution and subsequent extraction with dichloromethane yielded a yellow oil that was characterized by GC–MS and ¹H NMR spectroscopy. Two peaks were observed in the GC, one generated by the reactant (*p*-*tert*-butylphenol) and the other caused by a newly formed product. The mass spectrum of the latter shows the highest mass at *m/z* = 166. This signal is assigned to *p*-*tert*-butylcatechol. The mass spectrum of an authentic sample of this compound (as retrieved from the spectroscopic data base for organic compounds)^[48] shows a similar fragmentation pattern. The ¹H NMR spectrum of the yellow oil supports the formation of the *ortho*-dihydroxylated product. A yield of ca. 15% catechol was determined from the integrated intensity ratio of the *tert*-butyl proton signals in the mixture (reactant vs. product). In a second experiment, 5 equiv. of the phenol was used in a minimum amount of solvent. The same workup procedure yielded 30% product. Overall, these findings substantiate tyrosinase-like activity of the O-type species formed in the reaction of **8** with dioxygen.

Conclusions

This study describes the rich coordination chemistry of pyridine-derived polypodal polyamine ligands towards copper(I) and copper(II). All ligands have NN₄ donor sets of similar topology, but vary in terms of donor-set quality (primary vs. secondary vs. tertiary amines) and rigidity, or juxtapositional fixedness (polypodal vs. polycyclic ligands). The observed coordination geometries are determined by a combination of factors: ligand flexibility, steric demand of the donor-atom substituents and stereochemical preferences of the metal ion [copper(I) vs. copper(II)]. Structural distortions, typical of Cu^{II} complexes with more accommodating chelate ligands, are effectively suppressed in some cases, and polynucleating coordination modes are observed in others (both for Cu^I and for Cu^{II}). Not unexpectedly, ligand oxidation occurs when the copper(I) complexes of primary and secondary amine ligands used in this study are exposed to dioxygen. By contrast, the copper(I) complex of a “superpodal” Mannich base, which contains only tertiary amine donors in addition to an apical pyridine nitrogen atom, reacts with the formation of a dinuclear bis(μ-oxido)-copper(III) species after exposure to dioxygen at –90 °C under aprotic conditions, as indicated by its UV/Vis and resonance-Raman spectral characteristics. This product shows tyrosinase-like activity. We note that the present study has produced what is only the second example described in the literature of a bis(μ-oxido)dycopper(III) model complex that is capable of converting phenolate to catechol as the only product. Our findings further support the idea that a bis-

(μ-oxido)dycopper(III) core has relevance as an active intermediate in the catalytic cycle of tyrosinase.

Experimental Section

CAUTION! Although no problems were encountered in this work, transition-metal perchlorate complexes with organic ligands are potentially explosive and should be handled with precautions.

Materials and Instrumentation: Unless noted otherwise, all reactions were carried out in dry solvents under dry dinitrogen using standard Schlenk techniques, or in an MBraun inert-atmosphere drybox containing purified dinitrogen. Solvents were dried by standard methods. The precursors [Cu(CH₃CN)₄]PF₆ and **1** were synthesized according to published procedures.^[49,50] All other chemicals were purchased from Aldrich or Acros and used without further purification. NMR spectra were recorded with Bruker ARX 200, AV 400 or ARX 500 spectrometers (see also the section on VT measurements below). IR spectra were measured by using KBr disks with a Perkin–Elmer Spectrum 100 Series FTIR spectrometer. Mass spectrometry was carried out by using a Finnigan MAT95S instrument (EI) and an Orbitrap LTQ XL instrument (Thermo Scientific. ESI). GC–MS measurements were carried out with a Shimadzu GC-2010 gas chromatograph (30 m Rxi-5ms column) linked with a Shimadzu GCMA-QP 2010 Plus mass spectrometer. Elemental analyses were performed by combustion analysis using a Thermo Finnigan EAGER 300 (Flash 1112) apparatus. UV/Vis spectra were measured by using a Varian Cary 50 spectrometer equipped with a UV/Vis quartz immersion probe (light path 1 mm, Hellma), a home-built measuring cell and an immersion thermometer. Resonance Raman spectra were measured at 90 K (Resultec/Linkam cryostat) by using a confocal Raman microscope HR-800, Jobin Yvon. Samples were excited with the 413 nm laser line of a continuous-wave Kr⁺ laser (Innova 300, Coherent). The scattered light was collected over 180° through a lens (Olympus, 20×, NA 0.35) of the microscope setup. Light detection was performed by a nitrogen-cooled CCD camera. Elastic scattering and laser plasma lines were eliminated by means of a notch filter and an interference filter. The spectrometer operation was performed with the LabSpec software (v4.07, Dilor-Jobin Yvon-Spex). For the spectra calibration, a standard mercury lamp was used. Spectral resolution was better than ±0.5 cm⁻¹. The samples were prepared as follows: A droplet of the solution (freshly prepared at 193 K) was placed on an aluminium or gold disc and shock-frozen by direct immersion in liquid nitrogen. Photochemical degradation of the investigated complex was observed within a few seconds under the resonance conditions applied. For this reason, the working power of the laser was lowered considerably (500–600 μW). In addition to the low-power conditions, rotation of the sample allowed the probing of undamaged regions of the sample while the camera was open (2 s). Around 10–20 single spectra were averaged to improve the signal/noise ratio. The overall measuring time was between 20 and 40 s. After accumulation, the recorded spectra were manipulated by using the OPUS software (v5.5 or higher, Bruker Analytical Instruments). A baseline correction was done by using a polynomial function. In the case of the ¹⁸O₂-labelled sample, the signals of the residual ¹⁶O₂ species were subtracted manually before the baseline correction.

X-ray Diffraction: Data collection for complex **7** was performed with a Bruker Nonius KappaCCD diffractometer by using graphite-monochromated Mo-*K*_α radiation with λ = 0.71073 Å. The structure was solved by direct methods and refined by using the program SHELXTL NT 6.12.^[51] All non-hydrogen atoms were re-

fined anisotropically. Data collection for the remaining structures was performed with an Oxford Diffraction Xcalibur S instrument equipped with a Sapphire CCD-detector by using graphite-mo-chromated Mo- K_{α} radiation with $\lambda = 0.71073 \text{ \AA}$. Frames were integrated by using the SCALE3 ABSPACK algorithm. Structures were solved by direct methods using the program SHELXS-97. Subsequent full-matrix least-squares refinement of F_o^2 data was carried out by using SHELXL-97.^[52] All non-hydrogen atoms were refined anisotropically. Molecular graphics were created by using the software packages ORTEP-3 for Windows^[53] and MERCURY 2.3.^[54] Treatment of disorder: In complex **6**, the trifluoro acetate molecules show disorder in the CF₃ unit. Three orientations could be refined separately for each molecule [the occupancy factors are 27.2(4), 26.6(10) and 46.2(9) for atoms F(41)–F(43); 36.6(4), 34.8(9) and 28.6(9) for atoms F(51)–F(53); 44.0(4), 18.1(8) and 37.9(9) for atoms F61–F63; 45.1(4), 25.2(9) and 29.7(9) for atoms F(71)–F(73)]. Treatment of hydrogen atoms: Unless otherwise noted, hydrogen atoms were located on the difference Fourier map and placed in positions of optimized geometry. Isotropic displacement parameters were tied to those of the corresponding carrier atoms. For the refinement of the water hydrogen atoms [aqua ligand H(3A)–O(3)–H(3B) and water molecule H(4A)–O(4)–H(4B)] in compound **6**, H–O–H-angle, O–H-distance restraints and anisotropic displacement-factor constraints were used. The hydrogen atom H(80) of a methanol molecule in **6** was refined by using O–H-angle and O–H-distance restraints. The hydrogen atom positions H(5A) and H(5B) in compound **7** were obtained from a difference Fourier synthesis and refined with O–H-distance restraints. CCDC-827107 (**2**·4HCl·2H₂O), -827108 (**4**), -827109 (**5**), -827110 (**6**·6MeOH·2H₂O), -827111 (**7**) contain the supplementary crystallographic data for this paper. These data can be obtained free of charge from The Cambridge Crystallographic Data Centre via www.ccdc.cam.ac.uk/data_request/cif.

Computational Details: Initial geometries were constructed by using Avogadro^[55] and preoptimized by using the UFF method^[56] as implemented in OpenBabel.^[57] Subsequent DFT calculations were performed by using the programme Gaussian 03 (C02).^[58] The (restricted) hybrid functional B3LYP as implemented in the Gaussian package^[59] was used in combination with the DGauss basis set DGDZVP for geometry optimizations as well as numerical frequency calculations.^[60,61] This combination was chosen to provide a reasonable geometric description of the rather large copper(I) complex **8** at moderate computational cost.^[62,63] Geometries were optimized without constraints by using the default SCF procedure in Gaussian 03. Numerical frequency calculations were performed to characterize the structures either as minima (Nimag = 0; Nimag: number of imaginary frequencies) or saddle points (Nimag = 1). The transition state shown in Figure 9 is characterized by an imaginary frequency corresponding to a movement of all four pendant amine arms, coordinated and uncoordinated, in a skeletal deformation vibration. This vibration is antisymmetric with respect to the C_s symmetry plane present in the equilibrium geometry, which appears reasonable when assuming an enantiomerization proceeding through this saddle point.

VT NMR Measurements: Complex **8** was investigated in [D₈]THF in the range from room temperature to 180 K. Oxygen-free conditions were ensured by application of the freeze/pump technique under high vacuum to a fresh solvent aliquot that had been stored overnight over a freshly prepared potassium mirror. The solvent was condensed onto the solid sample in a Schlenk tube attached to a Schlenk line by using liquid nitrogen. After allowing the tube to warm to room temperature, the sample was heated to reflux and then transferred as a supersaturated solution to the NMR tube.

The copper(I) complex had precipitated almost completely (yellow solid) after the sealed tube had been allowed to stand for several days. This ensured saturation of the solution with the copper(I) complex and static conditions. NMR tubes were flame-sealed under high vacuum after the contents had been cooled to $-196 \text{ }^{\circ}\text{C}$. VT NMR spectra were measured by using a Bruker AvanceIII 500 spectrometer.

2-{6-[1,3-Bis(dimethylamino)propan-2-yl]pyridin-2-yl}-N¹,N¹,N³,N³-tetramethylpropane-1,3-diamine (2**):** The ligand was prepared according to a modified literature procedure.^[15] 2,6-Lutidine (75 g, 0.7 mol), dimethylamine hydrochloride (460 g, 5.6 mol) and para-formaldehyde (170 g, 5.6 mol) were suspended in water (500 mL) and refluxed for 24 h, which resulted in a clear brown solution. Water was distilled off (ca. 200 mL), and the remaining solution left to stand at room temperature. The colourless crystalline solid, which had precipitated after 4 weeks, was filtered, washed with a small amount of cold methanol and dried in vacuo (colourless solid, tetrahydrochloride dihydrate; 10.0 g; yield based on 2,6-lutidine: 3%). C₁₉H₄₅Cl₄N₅O₂ (515.23): calcd. C 44.11, H 8.77, N 13.54; found C 44.09, H 7.78, N 13.61. The free base was obtained by dissolving the hydrochloride in dry methanol and treating the solution with sodium methoxide (4 equiv.). The solvent was distilled off, the residue taken up in tetrahydrofuran and the suspension filtered. Evaporation of the solvent from the filtrate gave **2** as a colourless, highly viscous oil. ¹H NMR (400MHz, [D₆]DMSO, room temp.): $\delta = 7.47$ [t, ³J(H,H) = 7.7 Hz, 1 H, py-H⁴], 6.99 [d, ³J(H,H) = 7.3 Hz, 2 H, py-H^{3/5}], 3.07 [m, (9 lines), ³J(H, H) = 8.5, ³J(H, H) = 6.0, ²J(H, H) = 12.0 Hz, 2 H, bridgehead CH], 2.53 (m, 4 H, C-CH₂-N), 2.41 (m, 4 H, C-CH₂-N), 2.05 (s, 24 H, CH₃) ppm. {¹H} ¹³C NMR (100.6 MHz, [D₆]DMSO, room temp.): $\delta = 162.05$ (s, *ortho*-py-C), 135.65 (s, *para*-py-C), 120.47 (s, *meta*-py-C), 62.85 (s, CH₂), 45.47 (s, CH₃), 43.75 (s, CH) ppm. MS (ESI): $m/z = 336.31154$ [M + H]⁺.

N¹,N³,2-Trimethyl-2-{6-[2-methyl-1,3-bis(methylamino)propan-2-yl]pyridin-2-yl}propane-1,3-diamine (3a**):** 2·4HBr·MeOH (1.85 g, 3.04 mmol) was added to a saturated aqueous solution of K₂CO₃ (30 mL). The mixture was cooled to 0 °C, and ClCO₂Et (1.3 mL, 14.68 mmol) was added dropwise while stirring. Upon completion of the addition, the cooling bath was removed and the mixture stirred overnight. The mixture was extracted with ethyl acetate (3 × 30 mL), the organic phases were separated and dried with Na₂SO₄, and the solvent was removed with a rotary evaporator to obtain the crude carbamate intermediate (1.55 g, 94%). ¹H NMR (200 MHz, CDCl₃, room temp.): $\delta = 7.64$ [t, ³J(H,H) = 7.9 Hz, 1 H, py-H], 7.26 [d, ³J(H,H) = 7.9 Hz, 2 H, py-H], 5.73 [s (br), 4 H, NH], 4.09 [q, ³J(H,H) = 7.1 Hz, 8 H, O-CH₂-Me], 3.69–3.38 [ddd, ³J(H,H) = 7.6 Hz, ²J(H,H) = 5.8 Hz, 8 H, C-CH₂-N], 1.29 (s, 6 H, CH₃), 1.19 [t, ³J(H,H) = 7.1 Hz, 12 H, O-CH₂-CH₃] ppm. {¹H} ¹³C NMR (50.3 MHz, CDCl₃, room temp.): $\delta = 162.4$ (s, *ortho*-py-C), 157.4 (s, C=O), 137.1 (s, *para*-py-C), 118.9 (s, *meta*-py-C), 60.8 (s, O-CH₂-Me), 46.5 (s, Py-C-Me), 46.3 (s, CH₂), 21.5 (s, CH₃), 14.5 (s, O-CH₂-CH₃) ppm. IR (KBr): $\tilde{\nu} = 1036, 1139, 1249, 1463, 1540, 1577, 1701$ (C=O), 2935, 2980, 3336 cm⁻¹. MS (EI, 190 °C): m/z (%) = 102 (8) [CH₂NHCOOEt]⁺, 438 (100) [M – CH₂-NHCOOEt]⁺, 450 (15) [M – 2 OEt]⁺, 495 (10) [M – OEt]⁺, 540 (5) [M]⁺. C₂₅H₄₁N₅O₈ (539.62): calcd. C 55.64, H 7.66, N 12.98; found C 55.41, H 7.54, N 12.78. Reduction to **3a**: A solution of the carbamate (740 mg, 1.37 mmol) in THF (10 mL) was added dropwise to a suspension of lithium aluminium hydride (418 mg, 11 mmol) in THF (10 mL) over 10 min. The resulting suspension was refluxed for 17 h, during which time its colour changed from colourless through yellow to greenish. The mixture was allowed to cool and then carefully hydrolyzed at 0 °C by addition of water (2 mL)

and concd. aqueous NaOH (10 mL), to give an aqueous phase of strongly basic pH. The aqueous phase was extracted with THF (3 × 15 mL), and the combined organic phases were dried with Na₂SO₄. The crude product was isolated after solvent evaporation as a light yellowish oil (400 mg, 95%). ¹H NMR (400 MHz, CDCl₃, room temp.): δ = 7.56 [t, ³J(H,H) = 7.9 Hz, 1 H, py-*H*⁴], 7.13 [d, ³J(H,H) = 7.8 Hz, 2 H, py-*H*^{3/5}], 2.91 [dd, ²J(H,H) = 12.3 Hz, 8 H CH₂], 2.34 (s, 12 H, NH-CH₃), 1.34 (s, 6 H, CH₃) ppm.

Hexahydro-5-[6-(hexahydro-5-methylpyrimidin-5-yl)pyridin-2-yl]-5-methylpyrimidine (4): Paraformaldehyde (0.73 g, 22 mmol, 90–92%) was added in one portion to a stirred solution of **1** (2.77 g, 11 mmol) in methanol (15 mL). The colour of the solution immediately changed from yellow to colourless, and the aldehyde dissolved. The mixture was refluxed for 24 h. After cooling to room temperature, the solvent was removed in vacuo to yield a highly viscous yellowish oil. The crude product was recrystallized from toluene by diffusion of pentane to give **4** as colourless crystals (2.42 g, 80%). ¹H NMR (200 MHz, [D₆]DMSO, room temp.): δ = 7.69 [t, ³J(H,H) = 7.9 Hz, 1 H, py-*H*⁴], 7.24 [d, ³J(H,H) = 7.9 Hz, 2 H, py-*H*^{3/5}], 3.53 (s, 4 H, N-CH₂-N), 3.40 [d, ²J(H,H) = 13.3 Hz, 4 H, C-CH₂-N], 2.75 [d, ²J(H,H) = 13.3 Hz, 4 H, C-CH₂-N], 1.89 [t, ³J(H,H) = 6.5 Hz, 4 H, NH], 1.10 (s, 6 H, CH₃) ppm. {¹H}¹³C NMR (50.3 MHz, [D₆]DMSO, room temp.): δ = 164.9 (s, *ortho*-py-C), 137.5 (s, *para*-py-C), 118.2 (s, *meta*-py-C), 62.3 (s, CH₂), 55.5 (s, CH₂), 39.3 (s, CMe), 24.9 (s, py-CH₃) ppm. IR (KBr): ν̄ = 755, 815, 892, 941, 994, 1068, 1084, 1001, 1134, 1170, 1210, 1260, 1300, 1376, 1420, 1466, 1576, 1635, 2868, 2931, 2961, 3306, 3402 cm⁻¹. MS (EI, 70 eV): *m/z* (%) = 275 (10) [M]⁺. C₁₅H₂₅N₅ (275.40): calcd. C 65.42, H 9.15, N 25.43; found C 65.21, H 9.19, N 25.43.

[Cu(3)](ClO₄)₂ (5): Method a: A solution of hexakis(dimethylformamide)copper(II) perchlorate (406 mg, 0.58 mmol) in methanol (1 mL) was added dropwise to a solution of **3a** (180 mg, 0.58 mmol) in methanol (2 mL). The colour of the solution changed from colourless to dark blue, and it began to deposit a precipitate. Paraformaldehyde (38 mg, 1.16 mmol) was added in one portion and the reaction mixture stirred at room temperature for 14 h, during which time the colour turned to turquoise. Crude **5** (110 mg, 32%) was collected by filtration, washed with cold methanol and dried in vacuo. Slow concentration of a solution of **5** in acetonitrile yielded dark blue single crystals. Method b: Crystals of **5** were also obtained when the reaction sequence was inverted. Paraformaldehyde (47 mg, 0.71 mmol) was added in one portion to a solution of **4** (220 mg, 0.71 mmol) in methanol (2 mL). As the solid dissolved, hexakis(dimethylformamide)copper(II) perchlorate (500 mg, 1.43 mmol) in methanol (1 mL) was added dropwise. The reaction mixture was stirred at room temperature for 14 h, during which time the colour turned to turquoise. The crude product **5** (180 mg, 43%) was collected by filtration as a light blue solid, washed with cold methanol and dried in vacuo. Slow evaporation of the solvent from a solution of **5** in acetonitrile yielded dark-blue single crystals suitable for X-ray structure determination. IR (KBr): ν̄ = 523, 563, 623, 702, 769, 825, 858, 905, 931, 981, 1021, 1091, 1194, 1217, 1240, 1250, 1303, 1333, 1373, 1396, 1420, 1469, 1582, 1596, 1645, 2017, 2745, 2868, 2884, 2921, 2947, 2980, 3249, 3442 cm⁻¹. MS (ESI): *m/z* (%) = 197.1016 [Cu(3)]²⁺, 332.2817 [3 + H]⁺, 493.1517 [Cu(3)-ClO₄]⁺. C₁₉H₃₃Cl₂CuN₅O₈ (593.88): calcd. C 38.42, H 5.60, N 11.79; found C 38.65, H 3.65, N 11.51.

[Cu₆(4)₂(μ-CF₃CO₂)₂(CF₃CO₂)₄(H₂O)₂(μ₃-OH)₄](CF₃-CO₂)₂·6MeOH·2H₂O (6): Method A: Compound **4** (98 mg, 0.36 mmol) was dissolved in methanol (3 mL), and a solution of copper(II) chloride (52 mg, 0.39 mmol) in methanol (1 mL) was added dropwise. The addition was accompanied by a colour change

from colourless to dark green. In order to exchange the counterion, silver(I) trifluoroacetate (172 mg, 78 mmol) in methanol (1 mL) was added. This caused the colour of the solution to change to dark blue instantaneously, and silver chloride started to precipitate. The suspension was filtered and the filtrate concentrated by slow solvent evaporation. Dark blue crystals of **6** had formed after 3 d. Method B: The reproducibility of the formation of **6** was ascertained by a directed synthesis. A solution of copper(II) trifluoroacetate was prepared by mixing solutions of trifluoroacetic acid (5.1 mL, 66.4 mmol, 98%) in water (50 mL) and basic copper carbonate (3.67 g, 16.6 mmol) in water (10 mL). The concentration of copper(II) in the resulting solution was 0.56 mol L⁻¹. Ligand **4** (330 mg, 1.2 mmol) was then dissolved in methanol (5 mL), and an aliquot of the copper(II) trifluoroacetate solution (6.4 mL, 3.6 mmol, 0.56 M in water) was added dropwise to give a dark-blue solution. The pH value was adjusted to ca. 7–8 with aqueous sodium hydroxide (1 M) and the precipitate removed by filtration. The filtrate was set aside, and crystals of **6** formed by slow evaporation of the solvent after 2 d. Washing with cold methanol and hexane gave the pure product (390 mg, 34%). IR (KBr): ν̄ = 520, 609, 669, 709, 725, 762, 799, 818, 838, 901, 918, 981, 1001, 1044, 1137, 1204, 1277, 1327, 1360, 1390, 1436, 1579, 1596, 1675, 2891, 2980, 3153, 3286, 3406, 3562, 3671 cm⁻¹. MS (ESI): *m/z* = 276.2193 [4 + H]⁺. C₄₆H₅₄Cu₆F₂₄N₁₀O₂₀ (1903.80): calcd. C 29.01, H 2.86, N 7.36; found C 29.34, H 2.47, N 7.11.

[Cu(1)](PF₆) (7): A suspension of tetrakis(acetonitrile)copper(I) hexafluorophosphate (473.7 mg, 1.27 mmol) in THF (3 mL) was added dropwise to a stirred solution of **1** (320 mg, 1.27 mmol) in THF (3 mL). A yellow colour appeared immediately and the mixture deposited a yellow solid. The suspension was stirred for an additional 3 h, the solid collected by filtration, washed with THF and dried in vacuo (480 mg, 82%). ¹H NMR (500 MHz, [D₆]DMSO, room temp.): δ = 7.82 [t, ³J(H,H) = 7.9 Hz, 1 H, py-*H*⁴], 7.38 [d, ³J(H,H) = 8.0 Hz, 2 H, py-*H*^{3/5}], 3.00 [d, ²J(H,H) = 12.8 Hz, 4 H, C-CH₂-N], 2.88 [d, ²J(H,H) = 12.8 Hz, 4 H, C-CH₂-N], 2.70 [s (br), 8 H, NH₂], 1.26 (s, 6 H, CH₃) ppm. {¹H}¹³C NMR (125.8 MHz, [D₆]DMSO, room temp.): δ = 162.7 (s, *ortho*-py-C), 138.2 (s, *para*-py-C), 119.4 (s, *meta*-py-C), 49.7 (s, CH₂), 44.2 (s, C-Me), 22.2 (s, CH₃) ppm. IR (KBr): ν̄ = 559, 741, 749, 833, 915, 1004, 1018, 1074, 1446, 1466, 1567, 1577, 1615, 1980, 2838, 2884, 2951, 2974, 3052, 3341, 3379, 3383 cm⁻¹. MS (ESI): *m/z* (%) = 314.1400 [Cu(1)]⁺. C₁₃H₂₅CuF₆N₃P (459.88): calcd. C 33.95, H 5.48, N 15.23; found C 34.37, H 5.26, N 14.75.

[Cu(2)](PF₆) (8): A suspension of tetrakis(acetonitrile)copper(I) hexafluorophosphate (225 mg, 0.6 mmol) in THF (1 mL) was added dropwise to a stirred solution of **2** (202 mg, 0.6 mmol) in THF (3 mL). The colour of the solution turned to yellow-orange immediately, and stirring was continued for 2 h. The solvent was then removed in vacuo, and complex **8** was obtained as a yellow-brownish solid (300 mg, 98%). ¹H NMR (200 MHz, [D₆]DMSO, room temp.): δ = 7.84 [t, ³J(H,H) = 7.8 Hz, 1 H, py-*H*⁴], 7.27 [d, ³J(H,H) = 7.8 Hz, 2 H, py-*H*^{3/5}], 3.16 (m, 2 H, CH), 2.65 (m, 4 H, C-CH₂-N), 2.54 (m, 4 H, C-CH₂-N), 2.34 (s, 24 H, CH₃) ppm. {¹H}¹³C NMR (100.6 MHz, [D₆]DMSO, room temp.): δ = 161.1 (s, *ortho*-py-C), 137.2 (m, *para*-py-C), 120.5 (s, *meta*-py-C), 63.1 (s, CH₂), 46.7 (s, CH₃), 42.1 (s, CH) ppm. IR (KBr): ν̄ = 559, 619, 636, 755, 842, 991, 1038, 1101, 1144, 1164, 1190, 1244, 1267, 1293, 1373, 1413, 1466, 1576, 1596, 1655, 2731, 2775, 2824, 2844, 2868, 2901, 2947, 2974 cm⁻¹. MS (ESI): *m/z* (%) = 398.2337 [Cu(2)]⁺. C₁₉H₃₇CuF₆N₅P (544.04): calcd. C 41.95, H 6.85, N 12.87; found C 42.36, H 6.65, N 12.93.

[Cu(4)](PF₆) (9): A suspension of tetrakis(acetonitrile)copper(I) hexafluorophosphate (268 mg, 0.72 mmol) in THF (1 mL) was

Copper Complexes of "Superpodal" Amine Ligands

added dropwise to a stirred solution of **4** (220 mg, 0.79 mmol) in THF (2 mL). A yellow colour immediately appeared, and the solution deposited a yellow-greenish solid. Stirring was continued for 3 h, and the solid was then collected by filtration. Product **8** was washed with THF and dried in vacuo (260 mg, 75%). ¹H NMR (500 MHz, [D₆]DMSO, room temp.): δ = 7.89 [t, ³J(H,H) = 7.9 Hz, 1 H, py-H⁴], 7.53 [d, ³J(H,H) = 7.8 Hz, 2 H, py-H^{3/5}], 3.72 (s, 4 H, N-CH₂-N), 3.68 [dd, ²J(H,H) = 11.3 Hz, 4 H, C-CH₂-N], 2.83 [dd, ²J(H,H) = 11.3 Hz, 4 H, C-CH₂-N], 1.09 (s, 6 H, CH₃) ppm. {¹H}¹³C NMR (100.6 MHz, [D₆]DMSO, room temp.): δ = 163.8 (s, *ortho*-py-C), 138.6 (s, *para*-py-C), 120.8 (m, *meta*-py-C), 63.7 (m, CH₂), 56.0 (m, CH₂), 39.5 (s, C-Me), 27.3 (m, CH₃) ppm. IR (KBr): ν̄ = 559, 652, 739, 755, 842, 971, 998, 1064, 1104, 1170, 1244, 1297, 1333, 1356, 1383, 1463, 1576, 2871, 2934, 2961, 3070, 3283 cm⁻¹. MS (ESI): *m/z* (%) = 338.1407 [Cu(**4**)]⁺. C₁₅H₂₅CuF₆N₅P (483.85): calcd. C 37.23, H 5.21, N 14.47; found C 37.69, H 4.97, N 14.30.

Reaction of Complex 8 with Dioxygen To Produce 10: A Schlenk flask was charged with a solution of **8** in THF (1 mL), capped with a rubber septum and cooled to -90 °C by immersion in a liquid N₂/methanol bath. Dioxygen from an O₂ cylinder was then passed through the solution with a cannula. This caused the colour of the solution to change from yellowish green to a deep brown green. The oxygen flow was stopped after ca. 5 min. When using ¹⁸O₂ a three-way valve was employed to enable evacuation of the system before starting the oxygen flow, which was admitted into a previously set up static vacuum. Complex **10** may be stored for several hours at -90 °C under aprotic conditions. Upon warming to room temperature the solution undergoes a colour change to dark green, and **10** decomposes.

Reaction of Sodium *p*-tert-Butylphenolate: *p*-tert-Butylphenol (500 mg, 3.33 mmol) was dissolved in THF (5 mL), and a slight excess of sodium sand (80 mg, 3.48 mmol) was added in one portion. The mixture evolved gas, and its colour changed from colourless to light pink. The solution was separated from unreacted sodium with a cannula, and the solvent was removed in vacuo. Sodium *p*-tert-butylphenolate was obtained as a light-pink powder (567 mg, 99%). Method a: Complex **8** (75 mg, 0.14 mmol) in THF (30 mL) was exposed to O₂ as described above. Sodium *p*-tert-butylphenolate (24 mg, 0.14 mmol) dissolved in THF (1 mL) was added to the cooled solution of **10**, which caused an instantaneous colour change from yellow green to dark green. The reaction mixture was warmed to room temperature and subsequently quenched with aqueous HCl (30 mL, 1 M), resulting in a yellow solution. THF was removed in vacuo and the aqueous phase extracted with DCM (4 × 20 mL). The organic phases were combined, and the solvent was removed in vacuo to leave a yellow oil. GC-MS and ¹H NMR spectroscopy indicated the material to be a mixture of *p*-tert-butylphenol and *p*-tert-butylcatechol (in an approximate ratio of 85:15). Method b: The reaction was repeated by using a fivefold excess of sodium *p*-tert-butylphenolate. Complex **10** was prepared in the minimum amount of THF (3 mL). After acidic workup, the *p*-tert-butylphenol-derived mixture was again isolated as an oil. The conversion of the starting material was 30%, as concluded from ¹H NMR spectroscopic data.

Acknowledgments

Support of this work by the Deutsche Forschungsgemeinschaft (GR 1247/7-1) is gratefully acknowledged. We thank Dr. Anna Company for fruitful discussions, Ralf Reichert and Wiebke Matthes for assistance with NMR glassware, and Sebastian Kemper for technical assistance with the VT NMR spectroscopy.

- [1] B. Murphy, B. Hathaway, *Coord. Chem. Rev.* **2003**, *243*, 237–262.
- [2] D. Reinen, *Comments Inorg. Chem.* **1983**, *2*, 227–246.
- [3] B. J. Hathaway, *Struct. Bonding (Berlin)* **1984**, *57*, 55–118.
- [4] E. I. Solomon, J. W. Ginsbach, D. E. Heppner, M. T. Kieber-Emmons, C. H. Kjaergaard, P. J. Smeets, L. Tian, J. S. Woertink, *J. Chem. Soc. Faraday Trans.* **2011**, *148*, 11–39.
- [5] R. A. Himes, K. D. Karlin, *Curr. Opin. Chem. Biol.* **2009**, *13*, 119–131.
- [6] L. M. Mirica, X. Ottenwaelder, T. D. P. Stack, *Chem. Rev.* **2004**, *104*, 1013–1046.
- [7] E. A. Lewis, W. B. Tolman, *Chem. Rev.* **2004**, *104*, 1047–1076.
- [8] M. Roff, J. Schottenheim, G. Peters, F. Tuczec, *Angew. Chem.* **2010**, *122*, 6583; *Angew. Chem. Int. Ed.* **2010**, *49*, 6438–6422.
- [9] R. L. Peterson, R. A. Himes, H. Kotani, T. Suenobu, L. Tian, M. A. Siegler, E. I. Solomon, S. Fukuzumi, K. D. Karlin, *J. Am. Chem. Soc.* **2011**, *133*, 1702–1705.
- [10] J. Woertink, L. Tian, D. Maiti, H. R. Lucas, R. A. Himes, K. D. Karlin, F. Neese, C. Würtele, M. C. Holthausen, E. Bill, J. Sundermeyer, S. Schindler, E. Solomon, *Inorg. Chem.* **2010**, *49*, 9450–9459.
- [11] G. Chaka, J. L. Sonnenberg, H. B. Schlegel, M. J. Heeg, G. Jaeger, T. J. Nelson, L. A. Ochrymowycz, D. B. Rorabacher, *J. Am. Chem. Soc.* **2007**, *129*, 5217–5227.
- [12] A. Grohmann, *Dalton Trans.* **2010**, *39*, 1432–1440.
- [13] C. Zimmermann, F. W. Heinemann, A. Grohmann, *Eur. J. Inorg. Chem.* **2001**, 547–555.
- [14] D. H. Busch, *Chem. Rev.* **1993**, *93*, 847–860.
- [15] J. L. Hughes, Dissertation, University of Michigan, Ann Arbor, USA, **1961**.
- [16] H. A. Bent, *Chem. Rev.* **1961**, *61*, 275–311.
- [17] D. W. Gruenwedel, *Inorg. Chem.* **1968**, *7*, 495–501.
- [18] S.-D. Kim, J.-K. Kim, W.-S. Jung, *Bull. Korean Chem. Soc.* **1997**, *18*, 653–656.
- [19] H. Möhrle, M. Pycior, J. Lessel, *Sci. Pharm.* **1996**, *64*, 569–575.
- [20] Möhrle, M. Pycior, *Arch. Pharm.* **1995**, *328*, 293–296.
- [21] G. L. Buchanan, A. C. W. Curran, *Chem. Commun. (London)* **1966**, 773.
- [22] H. Kämpf, Dissertation, Technische Universität Berlin **2007**.
- [23] L. H. Gade, N. Mahr, *J. Chem. Soc., Dalton Trans.* **1993**, 489–494.
- [24] P. C. Bansal, I. H. Pitman, J. N. S. Tam, M. Martes, J. J. Kaminski, *J. Pharm. Sci.* **1981**, *70*, 850–854.
- [25] U. Salzner, *J. Org. Chem.* **1995**, *60*, 986–995.
- [26] Y.-Q. Zheng, D.-Y. Cheng, B.-B. Liu, W.-X. Huang, *Dalton Trans.* **2011**, *40*, 277–286.
- [27] F. Bramsen, A. D. Bond, C. J. McKenzie, R. G. Hazell, B. Moubaraki, K. S. Murray, *Chem. Eur. J.* **2005**, *11*, 825–831.
- [28] S. Triki, F. Thétiot, J. S. Pala, S. Golhen, J. M. Clemente-Juan, C. J. Gómez-García, E. Coronado, *Chem. Commun.* **2001**, 2172–2173.
- [29] J. A. Real, G. De Munno, R. Chiappetta, M. Julve, F. Lloret, Y. Journaux, J. C. Colin, G. Blondin, *Angew. Chem.* **1994**, *106*, 1223; *Angew. Chem. Int. Ed. Engl.* **1994**, *33*, 1184–1186; *Angew. Chem.* **1994**, *106*, 1223–1225.
- [30] X. Li, D. Cheng, J. Lin, Z. Li, Y. Zheng, *Cryst. Growth Des.* **2008**, *8*, 2853–2861.
- [31] X. Li, D. Cheng, J. Lin, Z. Li, Y. Zheng, *Cryst. Growth Des.* **2008**, *8*, 4602.
- [32] R. T. Azuah, L. R. Kneller, Y. Qiu, P. L. W. Tregenna-Piggott, C. M. Brown, J. R. D. Copley, R. M. Dimeo, *J. Res. Natl. Inst. Stand. Technol.* **2009**, *114*, 341.
- [33] W. J. Kasowski, J. C. Bailar Jr., *Polyhedron* **1994**, *13*, 1989–1996.
- [34] W. J. Kasowski, J. C. Bailar Jr., *Polyhedron* **1994**, *13*, 1997–2003.
- [35] D. A. Handley, P. B. Hitchcock, T. H. Lee, G. J. Leigh, *Inorg. Chim. Acta* **2001**, *314*, 14–21.

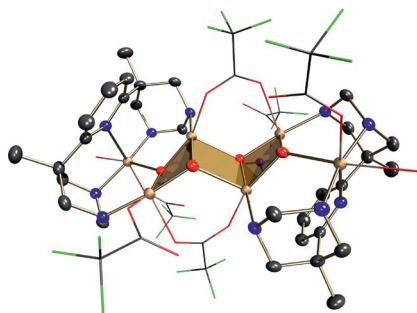
FULL PAPER

- [36] A. De la Lande, O. Parisel, H. Gerard, V. Moliner, O. Reinaud, *Chem. Eur. J.* **2008**, *14*, 6465–6473.
- [37] D. Utz, S. Kisslinger, F. Hampel, S. Schindler, *J. Inorg. Biochem.* **2008**, *102*, 1236–1245.
- [38] J. A. Halfen, S. Mahapatra, E. C. Wilkinson, S. Kaderli, V. G. Young Jr., L. Que Jr., A. D. Zuberbühler, W. B. Tolman, *Science* **1996**, *271*, 1393–1395.
- [39] L. Q. Hatcher, M. A. Vance, A. A. Narducci Sarjeant, E. I. Solomon, K. D. Karlin, *Inorg. Chem.* **2006**, *45*, 3004–3013.
- [40] E. I. Solomon, U. M. Sundaram, T. E. Machonkin, *Chem. Rev.* **1996**, *96*, 2563–2605.
- [41] A. P. Cole, V. Mahadevan, L. M. Mirica, X. Ottenwaelder, T. D. P. Stack, *Inorg. Chem.* **2005**, *44*, 7345–7364.
- [42] M. J. Henson, P. Mukherjee, D. E. Root, T. D. P. Stack, E. I. Solomon, *J. Am. Chem. Soc.* **1999**, *121*, 10332–10345.
- [43] M. Rolff, J. Schottenheim, H. Decker, F. Tuzcek, *Chem. Soc. Rev.* **2011**, *40*, 4077–4098.
- [44] L. M. Mirica, M. Vance, D. J. Rudd, B. Hedman, K. O. Hodgson, E. I. Solomon, T. D. P. Stack, *Science* **2005**, *308*, 1890–1892.
- [45] A. Company, S. Palavicini, I. Garcia Bosch, R. Mas-Ballesté, L. Que Jr., E. V. Rybak-Akimova, L. Casella, X. Ribas, M. Costas, *Chem. Eur. J.* **2008**, *14*, 3535–3538.
- [46] S. Herres-Pawlis, P. Verma, R. Haase, P. Kang, C. T. Lyons, E. C. Wasinger, U. Flörke, G. Henkel, T. D. P. Stack, *J. Am. Chem. Soc.* **2009**, *131*, 1154–1169.
- [47] I. Garcia-Bosch, A. Company, J. R. Frisch, M. Torrent-Sucarrat, M. Cardellach, I. Gamba, M. Güell, L. Casella, L. Que Jr., X. Ribas, J. M. Luis, M. Costas, *Angew. Chem.* **2010**, *122*, 2456; *Angew. Chem. Int. Ed.* **2010**, *49*, 2406–2409.
- [48] SDBSWeb, <http://riodb01.ibase.aist.go.jp/sdbs/>; National Institute of Advanced Industrial Science and Technology, viewed March **2011**.
- [49] G. J. Kubas, *Inorg. Synth.* **1990**, *28*, 68–70.
- [50] A. Grohmann, F. Knoch, *Inorg. Chem.* **1996**, *35*, 7932–7934.
- [51] Bruker Analytical X-ray Systems, *SHELXTL NT*, version 6.12, Bruker AXS GmbH, Karlsruhe, Germany, **2002**.
- [52] G. M. Sheldrick, *SHELXL-97*, Universität zu Göttingen, Göttingen, Germany, **1997**.
- [53] L. J. Farrugia, *J. Appl. Crystallogr.* **1997**, *30*, 565.
- [54] C. F. Macrae, I. J. Bruno, J. A. Chisholm, P. R. Edgington, P. McCabe, E. Pidcock, L. Rodriguez-Monge, R. Taylor, J. van de Streek, P. A. Wood, *J. Appl. Crystallogr.* **2008**, *41*, 466–470.
- [55] *Avogadro: an open-source molecular builder and visualization tool*, version 1.0, <http://avogadro.openmolecules.net/>.
- [56] A. K. Rappe, C. J. Casewit, K. S. Colwell, W. A. Goddard III, W. M. Skiff, *J. Am. Chem. Soc.* **1992**, *114*, 10024–10035.
- [57] N. M. O’Boyle, M. Banck, C. A. James, C. Morley, T. Vandermeersch, G. R. Hutchison, *J. Cheminf.* **2011**, *3*:33, DOI: 10.1186/1758-2946-3-33.
- [58] M. J. Frisch, G. W. Trucks, H. B. Schlegel, G. E. Scuseria, M. A. Robb, J. R. Cheeseman, J. A. Montgomery Jr., T. Vreven, K. N. Kudin, J. C. Burant, J. M. Millam, S. S. Iyengar, J. Tomasi, V. Barone, B. Mennucci, M. Cossi, G. Scalmani, N. Rega, G. A. Petersson, H. Nakatsuji, M. Hada, M. Ehara, K. Toyota, R. Fukuda, J. Hasegawa, M. Ishida, T. Nakajima, Y. Honda, O. Kitao, H. Nakai, M. Klene, X. Li, J. E. Knox, H. P. Hratchian, J. B. Cross, C. Adamo, J. Jaramillo, R. Gomperts, R. E. Stratmann, O. Yazyev, A. J. Austin, R. Cammi, C. Pomelli, J. W. Ochterski, P. Y. Ayala, K. Morokuma, G. A. Voth, P. Salvador, J. J. Dannenberg, V. G. Zakrzewski, S. Dapprich, A. D. Daniels, M. C. Strain, O. Farkas, D. K. Malick, A. D. Rabuck, K. Raghavachari, J. B. Foresman, J. V. Ortiz, Q. Cui, A. G. Baboul, S. Clifford, J. Cioslowski, B. B. Stefanov, G. Liu, A. Liashenko, P. Piskorz, I. Komaromi, R. L. Martin, D. J. Fox, T. Keith, M. A. Al-Laham, C. Y. Peng, A. Nanayakkara, M. Challacombe, P. M. W. Gill, B. Johnson, W. Chen, M. W. Wong, C. Gonzalez, and J. A. Pople, *Gaussian 03*, revision C.02, Gaussian, Inc., Wallingford, CT, USA, **2004**.
- [59] R. H. Hertwig, W. Koch, *Chem. Phys. Lett.* **1997**, *268*, 345–351.
- [60] J. Andzelm, E. Wimmer, *J. Chem. Phys.* **1992**, *96*, 1280–1303.
- [61] C. Sosa, J. Andzelm, B. C. Elkin, E. Wimmer, K. D. Dobbs, D. A. Dixon, *J. Phys. Chem.* **1992**, *96*, 6630–6636.
- [62] P. Aslanidis, P. J. Cox, A. Kaltzoglou, A. C. Tsipis, *Eur. J. Inorg. Chem.* **2006**, 334–344.
- [63] S. K. Hadjidakou, C. D. Antoniadis, P. Aslanidis, P. J. Cox, A. C. Tsipis, *Eur. J. Inorg. Chem.* **2005**, 1442–1452.

Received: November 11, 2011

Published Online: ■

Copper(I/II) complexes of varying nuclearity have been obtained with a series of tetrapodal pentadentate N-donor ligands.



A. Jozwiuk, E. A. Únal, S. Leopold,
J. P. Boyd, M. Haryono, N. Kurowski,
F. V. Escobar, P. Hildebrandt, J. Lach,
F. W. Heinemann, D. Wiedemann, E. Irran,
A. Grohmann* 1–15

Copper Complexes of “Superpodal”
Amine Ligands and Reactivity Studies
towards Dioxygen

Keywords: Tetrapodal pentadentate li-
gands / Copper / Dioxygen / Tyrosinase-
like activity / N ligands / Density functional
calculations